

## INVESTIGATION OF TRANSIENT COOLING OF AN AUTOMOBILE CABIN WITH A VIRTUAL MANIKIN UNDER SOLAR RADIATION

by

**Gokhan SEVILGEN\* and Muhsin KILIC**

Department of Mechanical Engineering, Faculty of Engineering and Architecture,  
Bursa, Uludag University, Turkey

Original scientific paper  
DOI: 10.2298/TSCI120623150S

*The aim of the paper is to present a three dimensional transient cooling analysis of an automobile cabin with a virtual manikin under solar radiation. In the numerical simulations the velocity and the temperature distributions in the automobile cabin as well as around the human body surfaces were computed during transient cooling period. The surface-to-surface radiation model was used for calculations of radiation heat transfer between the interior surfaces of the automobile cabin and a solar load model that can be used to calculate radiation effects from the Sun's rays that enter from the glazing surfaces of the cabin was used for solar radiation effects. Inhomogeneous air flow and non-uniform temperature distributions were obtained in the automobile cabin and, especially in ten minutes of cooling period, high temperature gradients were computed and measured and high temperature values were obtained for the surfaces which were more affected from the sunlight. Validations of the numerical results were performed by comparing numerical data with the experimental data presented in this study. It is shown that the numerical results were in good agreement with the experimental data.*

Key words: *computational fluid dynamics, automobile cabin, transient cooling, solar radiation*

### Introduction

Thermal comfort of the occupants in a vehicle cabin is a growing concern due to occupant's health and safety. In addition to that, with more stringent requirements for efficient utilisation of energy resources within the transport industry must rely on improving energy efficiency of vehicles [1, 2]. With this respect, engineers have to consider energy consumption during heating or cooling of an automobile cabin due to legal restrictions and efficient use of energy resources. The need to reduce heat loads that enter passenger compartments has become an important issue in the early stage of vehicle design and the radiation plays an important role on the thermal comfort in the compartment [3, 4]. Thus, engineers have to design more effective HVAC systems of automobiles under different environmental conditions. Computational fluid dynamics (CFD) analysis tool is now being used to evaluate the different environmental conditions of an automobile cabin in many aspects [3-17]. The experimental studies have been also performed under different environmental conditions [18-20]. But these studies were time consuming and the total costs of these studies were also very high. But, when the CFD tool is used with experimental studies such as wind tunnel tests, researchers have the ability to evaluate the thermal characteristics of the automobile cabin in different environmental conditions within a short time and CFD methods have also positive effects in the vehicle development time. For

\* Corresponding author; e-mail: gsevilgen@uludag.edu.tr

these reasons described, CFD method is a useful tool to determine 3-D velocity and temperature distributions, thermal characteristics of the automobile cabin, and the local heat transfer characteristics of the surfaces of the human body [16, 17]. Many researchers used CFD analysis tool as a complement to their experimental studies. Kilic and Sevilgen, [4] used different types of boundary conditions on the human body surfaces to determine the suitable boundary condition for evaluating thermal comfort. Numerical results were in good agreement with the experimental data used in their study. Zhang *et al.* [5, 6] investigated the environment simulation of an automobile with and without passengers and the comparisons between predicted and measured air temperatures were presented in their studies. However, the complexity of human thermo-physiological model and physiological shape of the human body and highly transient conditions in the vehicle cabin lead to difficulties in CFD analysis [7]. In this study, the flow field and the temperature distribution of the automobile cabin under the influence of solar radiation was carried out in transient cooling period. To evaluate the flow and the thermal characteristics of the vehicle cabin in different aspects, virtual points and planes in different locations were defined and the numerical results were compared to the experimental results. Thermal characteristics of the automobile cabin and human body surfaces were also considered in the numerical analysis. Solar radiation has been shown to cause considerable discomfort to people in vehicles [21]. The effects of solar radiation on surface temperature of the automobile cabin inside were discussed and the predicted transient temperature data were compared to the measured data obtained from the experimental study.

## Numerical simulation model and method

### Modelling geometry

The main surfaces and the interior of the automobile cabin are shown in fig. 1. This cabin was modelled by using dimensions of a real car which was a 2005 model Fiat Albea. In this automobile cabin, there are two types of inlet vents. These are defrost and console type inlet vents and they have rectangular shape. In this study, we just considered console type of inlet vents and we assumed that defrost type of inlet vents were turned off.

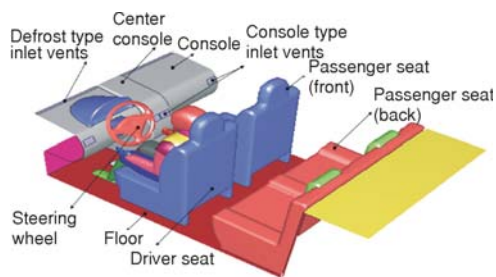


Figure 1. CAD model of the automobile cabin

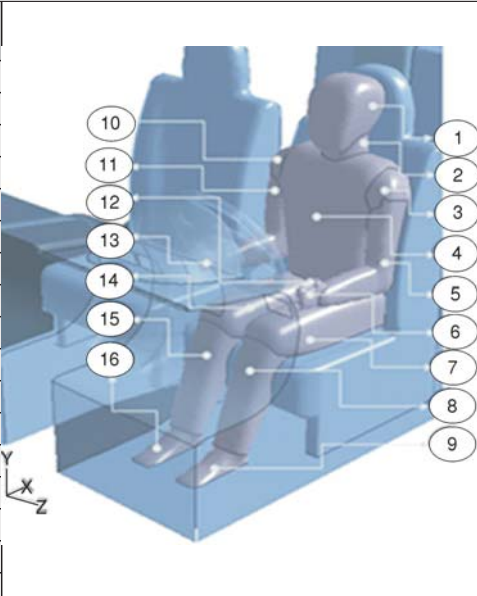
We designed a virtual manikin divided into 16 segments in sitting posture. This manikin was used in the numerical calculations to evaluate the local thermal characteristics of the human body and it had a standard height (1.70 m) and weight (70 kg), and it had a total surface area (1.81 m<sup>2</sup>) suitable for a standing posture and had a total surface area (1.20 m<sup>2</sup>) for a sitting posture. The rest of the total surface was contact with the solid surfaces of the automobile cabin. The main surfaces of the automobile cabin and the surfaces of the manikin used in this study were listed in tab.1.

### Computational domain and mesh structure

In previous research, Sevilgen and Kilic [8], used triangular elements on the surfaces of the automobile cabin and the tetrahedral cells in the volume region. In this study, we used hexcore meshing type which is a hybrid meshing scheme that include Cartesian cells inside the core of the computational domain and tetrahedral cells close to the boundary surfaces. This

**Table 1. Interior surfaces of the automobile cabin and the surfaces of the manikin**

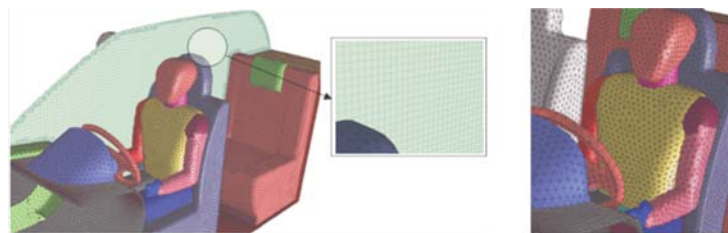
Surfaces of the automobile cabin	Surfaces of the manikin	Surface area [m <sup>2</sup> ]
Windshield	1 – Head	0.119
Rear glass	2 – Neck	0.020
Fdoor glass (rs)	3 – Lshoulder	0.016
Fdoor glass (ls)	4 – Chest	0.237
Bdoor glass (rs)	5 – Larm	0.113
Bdoor glass (ls)	6 – Lhand	0.018
Driver seat	7 – Lthigh	0.096
Passenger seat (f)	8 – Lleg	0.139
Passenger seat (b)	9 – Lfoot	0.027
Console	10 – Rshoulder	0.016
Centre console	11 – Rarm	0.113
Steering wheel	12 – Pelvis	0.005
Floor	13 – Rhand	0.018
Ceiling	14 – Rthigh	0.096
	15 – Rleg	0.139
	16 – Rfoot	0.027
	<b>Total</b>	<b>1.20</b>



Note: rs – right side; ls – left side; F, f – front; B, b – back; R – right; L – left

mesh structure was called “Hex-Core” and more detailed information about this mesh structure can be found in reference [22, 23]. The section view of volume cells at centre plane and the surface mesh of the automobile cabin are shown in fig. 2.

**Figure 2. The section view of volume cells at centre plane and surface mesh of the automobile cabin**



In the computational domain, about 900.000 volume cells were generated for the transient cooling simulation. This mesh structure was obtained from the comparison of the results of several numerical simulations to get optimum mesh density.

### Boundary conditions and solar simulation

The initial conditions used in this numerical study are shown in tab. 2. The exterior temperature of the numerical simulation was set to as a constant value of 30 °C and convective boundary condition was used for the outer and glass surfaces of the automobile cabin. The glass surfaces were defined as semi-transparent wall and the other outer surfaces were defined as opaque wall. In this study,

**Table 2. Initial conditions of the numerical simulation**

The initial cabin temperature	50 °C
The exterior temperature around the cabin	30 °C
Operating conditions (HVAC system)	Idle mode
Total simulation time and the time step	30 min/1 s

all glass surfaces in this passenger car have transmissivity of 80% and absorptivity of these walls is taken as 10% in the numerical simulations and the absorptivity of opaque surfaces is set to 80%. The convective heat transfer coefficient for external flow around the automobile cabin was set to 15 W/m<sup>2</sup>°C and the thickness of the glazing and solid walls are set as 5 mm and 12 mm, respectively. We assumed that the environmental conditions were remained unchanged during the numerical simulation. The initial air temperature inside the automobile cabin was set to 50 °C. The total simulation time was 30 min and at the beginning of the simulation, the simulation time step was set as 0.001 s and this value was constant for first 5 min of cooling time and it was set to 1 s for the rest of this numerical simulation. The time step is necessary for getting more precise and satisfactory numerical results, and choosing the time step correctly, especially at the beginning of the numerical simulation, affects the numerical results at the end of the simulation.

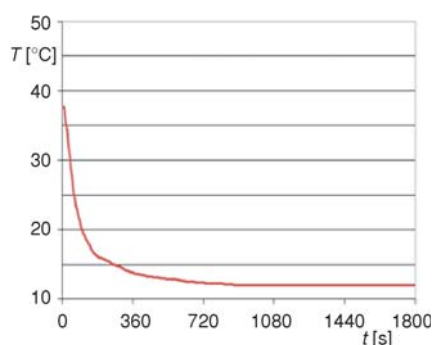


**Figure 3.** Transient temperature data for inlet vents

The air temperature at the inlet vents was determined as a function of time by means of a user defined function which was obtained from the measured data and this temperature profile shown in fig. 3 was used for all inlet vents in this numerical simulation. The velocity magnitude was set to 2.5 m/s for all inlet vents and the direction of the resultant velocity vector was normal to the surface boundary. Atmospheric conditions were applied at the outlet surface (tab. 3).

At the manikin surfaces we used temperature boundary condition and we assumed that the tempera-

**Table 3.** Solar radiation model and boundary conditions

Solar radiation model	
Solar radiation algorithm	Solar ray tracing algorithm
Radiation model	Surface to surface (S2S) model including view factors
Solar irradiation	875 W/m <sup>2</sup>
Boundary conditions	
Manikin surfaces	Constant surface temperature ( $T_{sc} = 33.7$ °C and $T_{sn} = 33.0$ °C)
Inlet vents (heat transfer)	Transient temperature profile obtained from measured data (fig. 3)
Inlet vents (momentum)	Constant velocity (2.5 m/s)
Outlet vents	Gauge pressure = 0 Pa
Exterior air temperature	30 °C
Glass surfaces	Convective boundary condition ( $h = 15$ W/m <sup>2</sup> °C), semi-transparent wall
Other outlet surfaces	Convective boundary condition ( $h = 15$ W/m <sup>2</sup> °C), opaque wall
Other inner surfaces	Adiabatic boundary condition

ture of manikin surfaces was constant and it was set to 33 °C at the naked surfaces such as head and hands, and at the clothed surfaces it was set to 33.7 °C as related to the thermal resistance of summer clothes. Heat interactions between human body and the immediate surroundings occur by several modes of heat exchange. Latent heat loss was not considered and respiration was neglected in the present computations. We assumed that the boundary conditions for the areas con-

tact with the solid surfaces were adiabatic thus we just considered the total sensible heat which is transferred from the human body surfaces to the environment by convection and radiation.

In this study FLUENT software was used for 3-D air flow and heat transfer field analysis. Fluent software solves continuum, energy and transport equations numerically with natural convection effects. In numerical solution, second order discretization method was used for convection terms and SIMPLE algorithm was chosen for pressure-velocity coupling. For the turbulence modelling, the RNG  $k-\epsilon$  model was chosen for the numerical calculations. This turbulence model is generally used for such calculations due to stability and precision of numerical results in literature [24, 25]. For including the solar simulation into the numerical simulation, we used solar load model which was available in FLUENT 6.3.26. This software provides a solar load model that can be used to calculate radiation effects from the Sun's rays that enter a computational domain. The position of the sun related to experimental conditions was determined with solar calculator available in FLUENT. In solar calculator, Sun's location in the sky was determined with a given time-of-day, date, and position and we defined the location of the cabin model with Cartesian co-ordinates and the sun direction vector considering the time of day and date of the experimental studies. The combining of all these parameters will produce a solar ray that would occur at that time for this location. In this study, the value of the direct normal solar irradiation produced in the solar load model was about  $875 \text{ W/m}^2$  at that given time for this numerical simulation. S2S radiation model including calculation of view factors was used for radiation heat transfer among the interior surfaces of the vehicle cabin. The detail description of these models can be found in reference [23].

### Experimental set-up

Experimental studies took place in Bursa, Turkey, on August. The tests were performed on 2005 model Fiat Albea sedan automobile equipped with  $1600 \text{ cm}^3$  engine. During the experiment both internal and external surface temperatures and interior air temperature measurements were taken. During the experiment only four of the console vents were fully opened. In addition, all measurements were taken in a parked automobile with only driver inside. To determine the interior air temperature distribution in the compartment, measurements were obtained from different level of the cabin. During the experiments, compartment internal surface temperatures such as; ceiling, front windshield, right and left windows, and internal body surface temperatures such as; seats, dashboard, instrument panel, and steering wheel were measured and recorded by 12 channel thermometer. Some points on which the measured data obtained in the test car are assigned in the volume of the virtual cabin and also on surfaces to validate the computed results. The locations of these points were described in tab. 4. Measurement devices are given in tab. 5. In order to de-

**Table 4. The location of the temperature sensors used in this study**

Points	Location	Points	Location
P1	Right front foot level	P4	Right back chest level
P2	Left front foot level	P5	Right back head level
P3	Right back knee level	P6	Left back knee level

**Table 5. Measurement devices**

	Measuring range	Accuracy
Temperature measurement Temperature probe	Cole palmer digi-sense 12 Channel thermometer $-200 + 300 \text{ }^\circ\text{C}$	0.1%
Velocity measurement Velocity probe	Testo 454 multi func. measurement device 0-10 m/s	0.02 m/s

termine the value of the experimental error, uncertainty analysis is carried out using equations proposed by Moffat [26]. Maximum uncertainties in experimental results were found to be within  $\pm 1\%$ . The test conditions were achieved after the automobile was kept waiting for two hours in the outer environment which had high temperature value and intense sunlight ( $1\text{kW/m}^2$ ).

### Results and discussions

The mean interior air temperature and the mean surface temperatures are shown in tab. 6. Mean surface temperature values ranged from  $38\text{ }^\circ\text{C}$  to  $56\text{ }^\circ\text{C}$  at 30 s of cooling period. At the beginning of the cooling period, the mean high surface temperature values were obtained at the console, steering wheel, center console, passenger seat (front), windshield surfaces, *etc.*, which were directly affected with the sunlight. The mean surface temperature values of the outer surfaces of the cabin such as windshield and glass surfaces were decreased slowly compared to the other surfaces which were not directly affected from the sunlight. On the other hand, the mean surface temperatures were continuously decreased with cooling time and the mean air temperature was computed about  $28\text{ }^\circ\text{C}$  at the end of the numerical simulation. Another result obtained

**Table 6. The computed mean surface temperature values and interior air temperature**

Cabin surfaces and interior air temperature	$T\text{ [}^\circ\text{C]}$						
	30 s	60 s	120 s	300 s	600 s	1200 s	1800 s
Windshield	47.8	46.5	44.4	43.1	42.4	42.0	41.5
Rearglass	39.8	37.9	36.0	34.2	33.0	33.3	31.6
Fdoor glass (rs)	41.3	38.9	37.3	35.5	35.0	34.3	34.5
Bdoor glass (rs)	38.0	35.9	33.7	31.9	31.2	31.3	30.9
Fdoor glass (ls)	39.7	38.2	36.3	35.0	34.2	34.0	33.9
Bdoor glass (ls)	38.4	36.7	34.4	32.9	31.7	31.3	31.4
Driver seat	45.4	42.0	37.0	34.2	33.0	33.0	32.4
Passenger seat (f)	53.8	50.3	44.7	41.3	40.7	39.4	39.3
Passenger seat (b)	46.1	41.8	37.3	33.3	31.8	34.4	31.6
Steering wheel	53.8	50.2	46.7	44.0	42.6	42.8	41.1
Console	55.7	52.7	48.0	45.6	44.3	43.0	42.7
Centre console	51.6	48.5	43.7	40.3	39.1	38.3	38.1
Cabinleftside	44.1	41.3	38.0	35.7	34.7	34.0	34.0
Cabinleftside	40.7	38.3	35.2	33.0	31.9	31.6	31.5
Floor	41.6	39.2	35.2	33.1	32.4	31.9	31.9
Ceiling	41.6	39.5	36.3	34.3	33.6	33.6	33.1
Interior air temperature	43.7	39.2	33.6	29.9	28.7	28.1	27.9

from these numerical simulations is that the front part of the cabin interior was more affected by the solar radiation than the rear part of the cabin. The surface temperature predictions of the numerical simulation were shown in fig. 4. At the beginning of the cooling period, the surface temperatures had very high values and the maximum temperature value was obtained for the console surface which was one of the more affected surfaces from the sunlight. This local temperature value for this surface was computed about  $72\text{ }^\circ\text{C}$  at 5 min of cooling period. These high temperature values occurred due to solar radiation and greenhouse effects in the automo-

bile cabin. The predicted surface temperature values at the rear part of the cabin interior were changed between 27 °C and 32 °C at 30 min of cooling period.

Air flow distribution of the vertical plane of the automobile cabin at 10 and 30 min of cooling periods were shown in fig. 5. At 30 min of cooling period, maximum air velocity was computed near the inlet vents (middle) and it was about 2.0 m/s. In accordance with flow direction this value was decreased to 0.83 m/s in the rear part of the cabin interior at that time. In the front region of the vertical plane of the automobile cabin, velocity values changed between 0.1 to 2.0 m/s while in the front region of this plane these values ranged from 0.1 to 1.33 m/s. From the comparison of the velocity distributions at 10 and 30 min of cooling periods, the velocity values computed for same locations at the vertical plane were changed

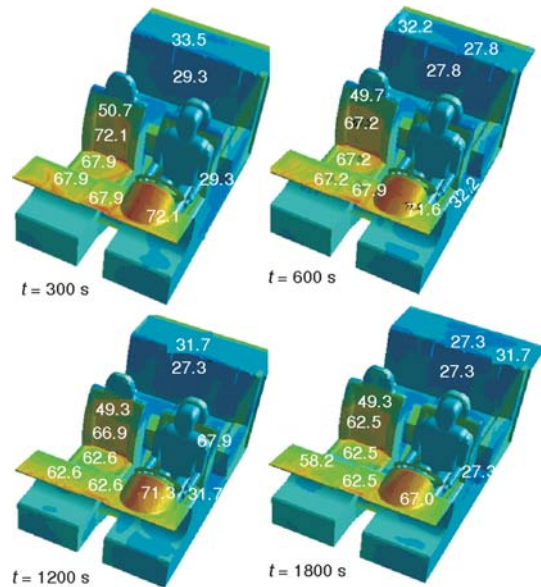


Figure 4. Local surface temperature [°C] predictions during cooling period

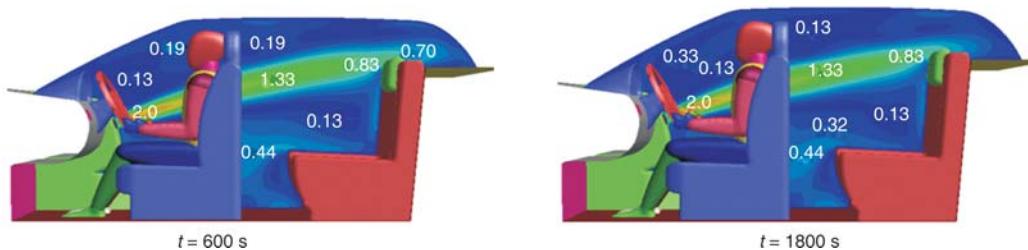


Figure 5. Velocity [ms] distributions at the vehicle vertical plane

slightly thus we conclude that the steady-state conditions were reached at 10 min of cooling period in terms of velocity distributions.

Air flow distribution of the horizontal plane of the automobile cabin at 10 and 30 min of cooling periods were shown in fig. 6. In the front region of the vertical plane, computed velocity values changed between 0.1 and 2.4 m/s. On the other hand, these values ranged from 0.1 to 0.3 m/s in the rear region of this plane. From these results, we can say that inhomogeneous velocity distribu-

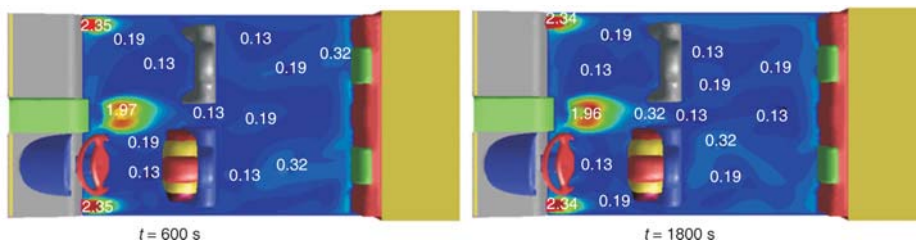
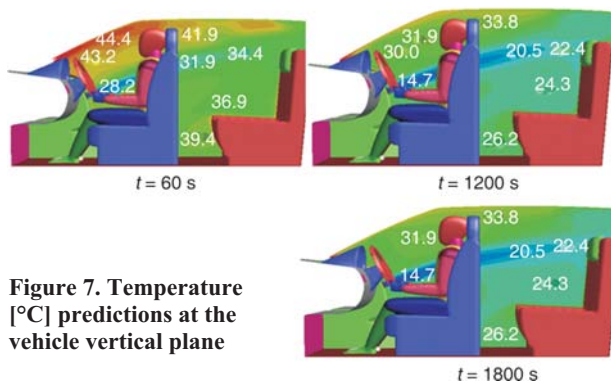
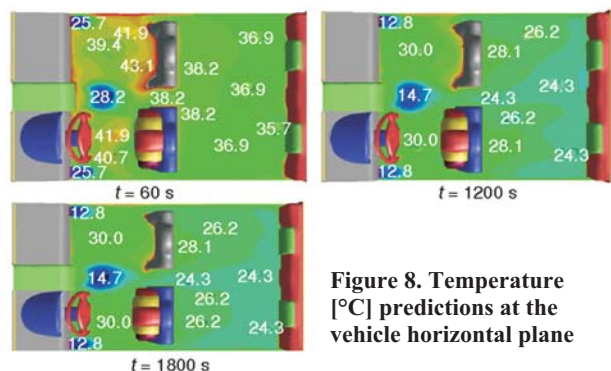


Figure 6. Velocity [ms<sup>-1</sup>] distributions at the vehicle horizontal plane



**Figure 7. Temperature [°C] predictions at the vehicle vertical plane**



**Figure 8. Temperature [°C] predictions at the vehicle horizontal plane**

and also around the human body surfaces. These temperature values were calculated about 42 °C and 43 °C, respectively, at one minute of cooling period. However, low temperature values occurred near the inlet vents and these temperature values were calculated about 28 °C at that time. At the rear part of the horizontal plane, computed local temperature values changed between 24 °C and 28 °C at 20 min of cooling period. These local values ranged from 13 °C to 30 °C in the front region of the horizontal plane. From these results it can be seen that the rear region of the vehicle cabin was cooled

more efficiently than the front region for this numerical simulation. tion occurred in the front region of this plane. Air temperature distributions at the vertical plane during cooling period were shown in fig. 7. High temperature values occurred near the driver head level and the windshield surface at the beginning of the cooling period due to solar radiation effects. The computed temperature values of the vehicle vertical plane ranged from 28 to 45 °C at 60 s of cooling period and these computed temperature values decreased continuously during cooling period. At 30 min of cooling period predicted temperature values at this plane changed between 15 °C and 34 °C. These results show that non-uniform air temperature distribution was obtained for the vertical plane of the vehicle cabin at 30 min of cooling period. Air temperature distributions at the horizontal plane were shown in fig. 8. At the beginning of the cooling period, high air temperature values were computed near the front passenger seat

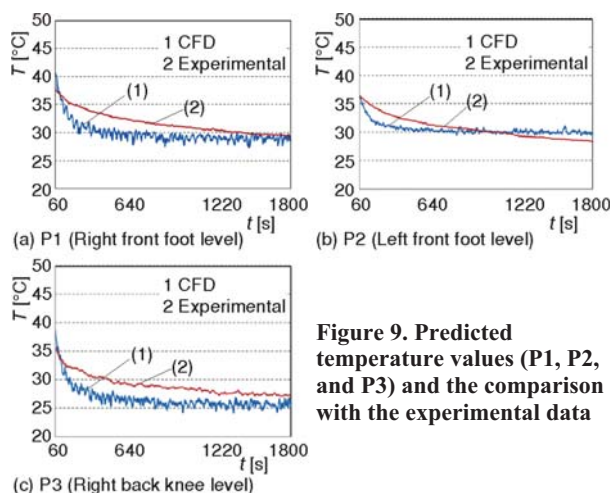


**Figure 9. Predicted temperature values (P1, P2, and P3) and the comparison with the experimental data**

Comparisons of the experimental data and predicted temperature values at measuring points located in the vehicle cabin environment are shown in figs. 9 and 10. It can be seen from the results at the selected points (P1, P2, P3, P4, P5 and P6), the temperature differences between predicted and measured data were about 2 °C in general. The predicted temperature results for all locations had same trend with the experimental data. These predicted results were affected by many factors such as solar radia-



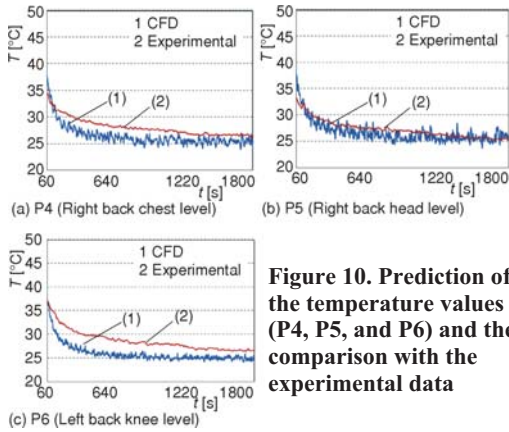


**Figure 10. Prediction of the temperature values (P4, P5, and P6) and the comparison with the experimental data**

**Table 7. The computed and measured surface temperature values**

Surfaces of the automobile cabin	Numerical $t = 1800$ s	Experimental $t = 1800$ s
Windshield	41.5	45.5
Rearglass	31.6	31.6
Fdoor glass (rs)	34.5	37.6
Fdoor glass (ls)	33.9	36.2
Passenger seat (f)	39.3	36.5
Steering wheel	41.1	38.1
Console	42.7	43.9
Ceiling	33.1	34.2

tion, material properties of automobile parts, metabolic heat production of the driver, heat losses from the outer surfaces of the cabin, heat transfer coefficient at the outer side, *etc.* Thus, the predicted results can be accepted as very good with confidence.

The computed and measured surface temperature values of the surfaces at 30 min of cooling period were listed in tab. 7. The predicted surface temperature values were in good agreement with the measured data in general.

### Conclusions

In this study, a 3-D transient turbulent flow simulation with solar radiation effects was performed and the validation of the numerical results was achieved by the comparison of the results to the experimental data presented in this study. As a result of these numerical simulations we can say that inhomogeneous air flow distributions were obtained in general. Another important result is that non-uniform temperature distributions obtained especially in 10 min of cooling period so that we conclude that highly transient conditions were occurred in 10-15 min of cooling period. On the other hand, the steady-state conditions were reached after 15 min of cooling period in terms of velocity and temperature distributions. Air temperature and surface temperature predictions were in good agreement with the experimental data in general. We also shown that an automobile parked facing the Sun, the air and the surfaces affected by solar radiation reached considerable temperatures such as about 70 °C for the console surface. In addition, these surface temperatures decreased slowly than the others because solar radiation effects remain unchanged during cooling process. These results are very important for reducing thermal load of the automobile cabin and improving the thermal comfort conditions in an automobile cabin. Reducing the thermal load of an automobile cabin considering thermal comfort and energy consumption of automobile HVAC system is the main objective of our later studies.

### Acknowledgments

The authors would like to acknowledge to the Scientific and Technological Research Council of Turkey (TUBITAK) for supporting this research under the project number of 105M262 and also to FIAT-TOFAS for providing the test car.

### References

- [1] Manojlović, A. V., *et al.*, Fleet Renewal: An Approach to Achieve Sustainable Road Transport, *Thermal Science*, 15 (2011), 4, pp. 1223-1236

- [2] Jović, J. J., Djorić, V. D., Application of Transport Demand Modelling in Pollution Estimation of a Street Network, *Thermal Science*, 13 (2009), 3, pp. 229-243
- [3] Huang, L., Han, T., Validation of 3-D Passenger Compartment Hot Soak and Cool-Down Analysis for Virtual Thermal Comfort Engineering, SAE paper 2002-01-1304, 2002
- [4] Kilic, M., Sevilgen, G., Evaluation of Heat Transfer Characteristics in an Automobile Cabin with a Virtual Manikin during Heating Period, *Numerical Heat Transfer, Part A: Applications*, 56 (2009), 6, pp. 515-539
- [5] Zhang, H., et al., Studies of Air-Flow and Temperature Fields Inside a Passenger Compartment for Improving Thermal Comfort and Saving Energy, Part I: Test/Numerical Model and Validation, *Applied Thermal Engineering*, 29 (2009), 10, pp. 2022-2027
- [6] Zhang, H., et al., Studies of Air-Flow and Temperature Fields Inside a Passenger Compartment for Improving Thermal Comfort and Saving Energy, Part II: Simulation Results and Discussion, *Applied Thermal Engineering*, 29 (2009), 10, pp. 2028-2036
- [7] Ambs, R., Improved Passenger Thermal Comfort Prediction in the Preprototype Phase by Transient Interior CFD Analysis Including Mannequins, SAE paper 2002-01-0514, 2002
- [8] Sevilgen, G., Kilic, M., Transient Numerical Analysis of Airflow and Heat Transfer in a Vehicle Cabin During Heating Period, *International Journal of Vehicle Design*, 52 (2010), 1-4, pp. 144-159
- [9] Sevilgen, G., Kilic, M., Three Dimensional Numerical Analysis of Temperature Distributions in An Automobile Cabin, *Thermal Science*, 16 (2012), 1, pp. 321-326
- [10] Kilic, M., Sevilgen, G., Modelling Airflow, Heat Transfer and Moisture Transport Around a Standing Human Body by Computational Fluid Dynamics, *International Communications in Heat and Mass Transfer*, 35 (2008), 9, pp. 1159-1164
- [11] Han, T., et al., Assessment of Various Environmental Thermal Loads on Passenger Thermal Comfort, SAE paper 2010-01-1205, 2010
- [12] Jang, H., et al., 3-D Numerical and Experimental Analysis for Airflow within a Passenger Compartment, *International Journal of Automotive Technology*, 9 (2008), 4, pp. 437-445
- [13] Han, T., et al., Virtual Thermal Comfort Engineering, SAE paper, 2001-01-0588, 2001
- [14] Han, T., Chen, K., Assessment of Various Environmental Thermal Loads on Passenger Compartment Soak and Cool-Down Analyses, SAE paper 2009-01-1148, 2009
- [15] Mezrhab, A., Bouzidi, M., Computation of Thermal Comfort Inside a Passenger Car Compartment, *Applied Thermal Engineering*, 26 (2006), 14-15, pp. 1697-1704
- [16] Kilic, M., Sevilgen, G., The Effects of Using Different Type of Inlet Vents on the Thermal Characteristics of the Automobile Cabin and the Human Body During Cooling Period, *The International Journal of Advanced Manufacturing Technology*, 60 (2012), 5-8, pp. 799-809
- [17] Sevilgen, G., Kilic, M., Numerical Analysis of Airflow, Heat Transfer, Moisture Transport and Thermal Comfort in a Room Heated by Two-Panel Radiators, *Energy and Buildings*, 43 (2011), 1, pp. 137-146
- [18] Kaynakli, O., et al., Thermal Comfort During Heating and Cooling Periods in an Automobile, *Heat and Mass Transfer*, 41 (2005), 5, pp. 449-458
- [19] Kilic, M., Kaynakli, O., An Experimental Investigation on Interior Thermal Conditions and Human Body Temperatures during Cooling Period in Automobile, *Heat and Mass Transfer*, 47 (2011), 4, pp. 407-418
- [20] Tounsi, N., et al., Volumetric 3-Component Velocimetry Measurements of the Flow Field on the Rear Window of a Generic Car Model, *Thermal Science*, 16 (2012), 1, pp. 310-320
- [21] Parsons, K. C., Human Thermal Environments, Taylor & Francis, London, 2003, pp. 248-256
- [22] \*\*\*, Tgrid 5 User's Guide April 15, ANSYS, Inc., 2008
- [23] \*\*\*, Fluent 6 User's Guide, Fluent Inc., Lebanon, N. H., USA, 2001
- [24] Chen, Q., Comparison of Different  $k-\epsilon$  Models for Indoor Airflow Computations, *Numerical Heat Transfer, Part B*, 28 (1999), 3, pp. 353-369
- [25] Costa, J. J., et al., Test of Several Versions for the  $k-\epsilon$  Type Turbulence Modeling of Internal Mixed Convection Flows, *International Journal of Heat and Mass Transfer*, 42 (1999), 23, pp. 4391-4409
- [26] Moffat, R. J., Describing the Uncertainties in Experimental Results, *Experimental Thermal and Fluid Science*, 1 (1988), 1, pp. 3-17

Paper submitted: June 23. 2012

Paper revised: July 11, 2012

Paper accepted: July 20.2012